

**On the Spectrum and Nature of the Peculiar Type Ia Supernova  
1991T**

ADAM FISHER, DAVID BRANCH, KAZUHITO HATANO, and E. BARON

Department of Physics and Astronomy, University of Oklahoma, Norman, OK 73019–0225,  
USA

Received \_\_\_\_\_; accepted \_\_\_\_\_

## ABSTRACT

A parameterized supernova synthetic-spectrum code is used to study line identifications in the photospheric-phase spectra of the peculiar Type Ia SN 1991T, and to extract some constraints on the composition structure of the ejected matter. The inferred composition structure is not like that of any hydrodynamical model for Type Ia supernovae. Evidence that SN 1991T was overluminous for an SN Ia is presented, and it is suggested that this peculiar event probably was a substantially super-Chandrasekhar explosion that resulted from the merger of two white dwarfs.

*Subject headings:* radiative transfer — supernovae: individual (SN 1991T) — supernovae: general

## 1. Introduction

SN 1991T was a well observed and spectroscopically peculiar Type Ia supernova (Filippenko et al. 1992; Ruiz–Lapuente et al. 1992; Phillips et al. 1992; Branch, Fisher, & Nugent 1993). Before and around the time of maximum light its optical spectrum showed strong lines of Fe III rather than the usual SN Ia lines of singly ionized elements of intermediate mass, and although the deep red Si II absorption that is characteristic of SNe Ia finally did develop after maximum light, it never reached its usual strength.

In this paper we report the results of a study of photospheric–phase spectra of SN 1991T using the parameterized supernova spectrum–synthesis code SYNOW (Fisher et al. 1997; Fisher 1998). In Section 2, previous studies of the optical spectra of SN 1991T are briefly summarized. Our method of “direct” spectral analysis is described in Section 3, and results are presented in Section 4. In Section 5 we discuss evidence that SN 1991T was too luminous to be a Chandrasekhar–mass explosion, and suggest that it probably was a substantially super–Chandrasekhar explosion resulting from the merger of two white dwarfs. A general discussion appears in Section 6.

## 2. Previous Studies of SN 1991T Spectra

Filippenko et al (1992) presented optical spectra obtained from  $-12$  to  $+47$  days. (Throughout this paper, epochs are in days with respect to the date of maximum light, 1991 April 28; Lira et al. 1998). They showed that although the premaximum optical spectra did not resemble those of any other supernova, beginning near maximum light the usual SN Ia lines of intermediate–mass elements slowly developed, and months after explosion the iron–dominated spectrum appeared almost identical to that of a typical SN Ia. They identified the two strong features in the premaximum optical spectrum with

the Fe III  $\lambda 4404$  and  $\lambda 5129$  multiplets and concluded that the composition of the outer layers was dominated by iron–group elements. Given their inferred composition structure of a thin layer of intermediate–mass elements sandwiched between inner and outer regions dominated by iron–peak elements, they favored a double–detonation model (the nearly complete incineration of a mildly sub–Chandrasekhar–mass white dwarf by detonation waves propagating inward and outward from the base of an accumulated helium layer) for the origin of SN 1991T. They noted that it was odd, then, that in their +6 day spectrum an absorption near  $7550\text{\AA}$  that is ordinarily attributed to O I  $\lambda 7773$  seemed to be present at its usual strength.

Ruiz–Lapuente et al (1992) presented optical spectra obtained on seven consecutive nights from  $-13$  to  $-7$  days. They too identified the Fe III lines, as well as lines of Ni III, and they too concluded that the outer layers had undergone complete burning to iron–peak elements. They supported that conclusion by presenting synthetic spectra based on approximate NLTE calculations, for the time–dependent nickel–cobalt–iron composition that results from the radioactive decay of initially pure  $^{56}\text{Ni}$ . As they noted, though, the lines in their synthetic spectra tended to be stronger than the observed lines. Their spectra did not extend late enough in time for them to encounter the oxygen line. They did, however, discuss another puzzle. Their spectra showed no evidence for the high velocities of the outer layers that would follow from complete burning to iron–peak elements. They suggested that the line–forming layers had been decelerated upon encountering a low–density carbon–oxygen envelope associated with a merger of two white dwarfs.

Phillips et al. (1992) presented optical spectra obtained from  $-13$  to  $+66$  days. From the appearance of the spectra they concluded that the abundances of silicon, sulfur, and calcium in the outer layers were unusually low, but they did not specify what was present in their place.

Jeffery et al. (1992) carried out parameterized synthetic-spectrum calculations, based on the Sobolev approximation, an approximate radiative-equilibrium temperature distribution, and full LTE, including a Planckian rather than a resonance scattering source function. They modified the composition structure of the carbon-deflagration model W7 (Nomoto, Thielemann, & Yokoi 1984; Thielemann, Nomoto, & Yokoi 1986), by trial and error, to get reasonable fits to observed optical (and some IUE near-ultraviolet) spectra obtained at  $-9$ ,  $-3$ , and  $+10$  days. The adopted composition (displayed in their Figure 7) was complex, and not simply dominated in the outer layers by iron-peak elements. It was like that of model W7 for ejection velocities less than  $8500 \text{ km s}^{-1}$ ; heavily modified between  $8500$  and  $14,400 \text{ km s}^{-1}$  in favor of iron-peak elements at the expense of intermediate-mass elements; heavily modified between  $14,400$  and  $21,000 \text{ km s}^{-1}$  in favor of both intermediate-mass and iron-peak elements at the expense of carbon; and primarily carbon and oxygen above  $21,000 \text{ km s}^{-1}$ . Noting that somewhat weaker Fe III lines might have gone unrecognized in previous studies of other SNe Ia, they suggested that although the composition structure was unusual the explosion history of SN 1991T probably was not fundamentally different from that of a normal SN Ia.

Mazzali, Danziger, & Turatto (1995) also carried out parameterized spectrum calculations, using a Monte Carlo code and a resonance scattering source function. They were restricted to using a homogeneous composition above the photosphere at each of the seven epochs considered. For each epoch they used a combination of a mixed W7 composition and the time-dependent  $^{56}\text{Ni}$ -decay composition. They concluded that an unusually high temperature was partly responsible for the weakness of the lines of singly ionized intermediate-mass elements, but also that iron-peak elements dominated the composition above  $13,000 \text{ km s}^{-1}$ . They favored a “late-detonation” (Yamaoka et al. 1992) explosion mechanism in a Chandrasekhar-mass white dwarf for the origin of SN 1991T. (Mazzali et al referred to it as a “delayed detonation”, but by custom that term is used to

refer a class of models that, unlike the late detonations, do not synthesize  $^{56}\text{Ni}$  in the outer layers; e.g., Khokhlov, Müller, & Höflich 1993).

Nugent et al. (1995) calculated detailed NLTE spectra using the PHOENIX code [cf. Hauschildt and Baron 1998, and references therein], for a fixed composition (W7 mixed above  $8000 \text{ km s}^{-1}$ , with titanium enhanced by a factor of 10) and a series of temperatures. They found that their series of synthetic spectra gave a good account of many of the spectral differences among SNe Ia, from the peculiar, cool, “weak” SN 1991bg, through the normal SNe Ia, to the peculiar, warm, “strong” SN 1991T. This showed that to a certain extent the differences between the spectra of SNe Ia are due to temperature differences, and confirmed that in SN 1991T a high temperature can enhance the Fe III and Si III lines and weaken the lines of singly ionized elements. Still, the temperature differences among SNe Ia presumably are caused by differences in the amounts of ejected  $^{56}\text{Ni}$ , and differences in the composition structures certainly are to be expected.

### 3. Spectrum Synthesis Procedure

In this paper we use the fast, parameterized, supernova spectrum–synthesis code SYNOW to make a “direct” analysis (Fisher et al. 1997) of spectra of SN 1991T. The goal is to study line identifications and determine intervals of ejection velocity within which the presence of lines of various ions are detected, without initially adopting any particular composition structure. The composition and velocity constraints that we obtain with SYNOW then can provide guidance to those who compute hydrodynamical explosion models and to those who carry out computationally intensive NLTE spectrum modeling. The SYNOW code was described briefly by Fisher et al. (1997) and in detail by Fisher (1998). In our work on SN 1991T we have made extensive use of the paper by Hatano et al. (1998), which presented plots of LTE Sobolev line optical depths versus temperature for six

different compositions that might be expected to be encountered in supernovae, and which presented SYNOW optical spectra for 45 individual ions that can be regarded as candidates for producing identifiable spectral features in supernova spectra.

Fisher et al. (1997) concentrated on a high quality spectrum of the normal Type Ia SN 1990N that was obtained by Leibundgut et al. (1991) at  $-14$  days. Fisher et al. suggested that at this very early phase an absorption feature observed near  $6040\text{\AA}$ , which previously had been attributed to moderately blueshifted Si II  $\lambda 6355$ , actually was produced by highly blueshifted ( $v > 26,000 \text{ km s}^{-1}$ ) C II  $\lambda 6580$ , indicating the presence of an outer high-velocity carbon-rich layer in SN 1990N. In this paper we suggest that SN 1991T also contained an outer carbon-rich layer, but extending to lower velocity than in SN 1990N.

We have studied spectra of SN 1991T ranging from  $-13$  days to  $+59$  days. For comparison with each observed spectrum we have calculated a large number of synthetic spectra with various values of the fitting parameters. These include:  $T_{bb}$ , the temperature of the underlying blackbody continuum;  $T_{exc}$ , the excitation temperature;  $v_{phot}$ , the velocity of matter at the photosphere; and  $v_{max}$ , the maximum ejection velocity. For each ion that is introduced, the optical depth of a reference line also is a fitting parameter, with the optical depths of the other lines of the ion are calculated assuming Boltzmann excitation at  $T_{exc}$ . In addition, we can introduce restrictions on the velocity interval within which an ion is present; when the minimum velocity assigned to an ion is greater than the velocity at the photosphere, the line is said to be detached from the photosphere. The radial dependence of the line optical depths is taken to be exponential with e-folding velocity  $v_e = 3000 \text{ km s}^{-1}$  (with one exception to be discussed in section 4.2) and the line source function is taken to be that of resonance scattering. The most interesting fitting parameters are  $v_{phot}$ , which as expected, decreases with time, and the individual ion velocity restrictions, which constrain the composition structure.

## 4. Spectrum Synthesis Results

In this section we present comparisons of synthetic spectra with observed spectra at several selected epochs, to illustrate how we reach our conclusions about the composition structure of the ejecta. The premaximum and postmaximum spectra are discussed separately, because the the former were so peculiar while the latter became increasingly normal.

### 4.1. Premaximum

In the premaximum spectra only two features have obvious identifications: two strong features produced by the Fe III  $\lambda 4404$  and  $\lambda 5129$  multiplets. Figure 1 compares a  $-13$  day observed spectrum to a synthetic spectrum that has  $v_{phot} = 15,000$  km s $^{-1}$  and  $T_{exc} = 13,000$  K. The optical depth of the Fe III reference line and the velocity at the photosphere have been chosen such that the  $\lambda 5129$  multiplet gives a reasonable fit to the strong P Cygni feature near  $5000\text{\AA}$ . Similarly, the optical depth of the reference line of Ni III has been chosen to give a reasonable fit to the weaker absorption near  $5300\text{\AA}$ ; then, in the synthetic spectrum, Ni III also is responsible for the weak absorption near  $4700\text{\AA}$ . We consider the presence of Ni III lines in the observed spectrum to be probable.

The diagnostic value of a spectral feature is not simply proportional to its strength. A weak feature in the premaximum spectra that is of special interest to us is the broad, shallow absorption near  $6300\text{\AA}$ , which definitely is a real feature because it can be seen in almost all of the spectra obtained by Filippenko et al. (1992), Ruiz-Lapuente et al. (1992) and Phillips et al. (1992) earlier than  $-6$  days; this feature was not mentioned in the previous discussions of the SN 1991T spectra. As shown in Figure 1, C II  $\lambda 6580$  can account for this feature, and in spite of searching for a plausible alternative with the help



of the plots of Hatano et al. (1998), we have none to offer.

Figure 2 compares a  $-4$  day observed spectrum to a synthetic spectrum that has  $v_{phot} = 10,000 \text{ km s}^{-1}$  and  $T_{exc} = 13,000 \text{ K}$ . The two strong Fe III features are fit reasonably well, and Ni III and Ni II probably account for some of the other observed features. Additional ions of iron-peak elements would need to be introduced to account for the observed flux deficiency at  $\lambda < 3500 \text{ \AA}$ . The narrow absorption near  $4400 \text{ \AA}$  is well fit by the Si III  $\lambda 4560$  multiplet, which is the strongest optical multiplet of Si III and was identified in SN 1991T by Jeffery et al. (1992). Note that at this phase, there is a weak absorption near  $6200 \text{ \AA}$ , rather than the  $6300 \text{ \AA}$  of earlier phases. In general, supernova absorption features shift redward as the photosphere recedes with respect to the matter, or they remain unshifted if the line has become detached. A blueward shift of an absorption is almost a sure sign that a new line is beginning to make a significant contribution. In this case the new line is very likely Si II  $\lambda 6355$ , which in normal SNe Ia is very strong at this phase. (In the synthetic spectrum, lines of Ni II and Fe III also are affecting this feature.)

From the premaximum spectra we infer that iron, silicon, and probably nickel were present above  $10,000 \text{ km s}^{-1}$ , with iron being detected up to  $20,000 \text{ km s}^{-1}$ . If the nickel identifications are correct, then freshly synthesized iron-peak elements were present in these outer layers. Carbon seems to have been present down to at least  $15,000 \text{ km s}^{-1}$ . Between  $-13$  and  $-4$  days, the red absorption feature apparently transformed from mainly C II forming above about  $15,000 \text{ km s}^{-1}$  to mainly Si II forming above  $10,000 \text{ km s}^{-1}$ . A very careful study of a good series of spectra obtained within this time interval might better determine the minimum velocity at which C II was present. If the C II line became detached before the Si II line made its appearance, the observed absorption minimum would have remained constant at the detachment velocity until the development of the Si II line started to cause a shift to the blue.

## 4.2. Postmaximum

Figure 3 shows a +6 day observed spectrum. By this time the spectrum had begun to look much less peculiar. The synthetic spectrum has  $v_{phot} = 9500 \text{ km s}^{-1}$  and  $T_{exc} = 10,000 \text{ K}$ . The synthetic feature near  $5000\text{\AA}$  is now a blend of Fe III and Fe II lines. The observed S II and Si II features are weaker and narrower than in normal SNe Ia. In the synthetic spectrum of the top panel, a maximum velocity of  $12,000 \text{ km s}^{-1}$  for S II lines has been introduced to fit the absorptions near  $5300$  and  $5500\text{\AA}$ , and a maximum velocity of  $15,000 \text{ km s}^{-1}$  has been used to fit the Si II absorption near  $6200 \text{ \AA}$ . The lower panel shows how the fit degrades when these maximum velocities are not used.

The observed spectrum that appears in Figures 4 and 5 was obtained by Meikle et al. (unpublished) at +59 days. The synthetic spectra have  $v_{phot} = 4000 \text{ km s}^{-1}$  and  $T_{exc} = 10,000 \text{ K}$ . The upper panel of Figure 4 shows that resonance scattering by permitted lines of just three ions — Fe II, Ca II, and Na I — can give a reasonable account of most of the features in the observed spectrum, although the height of the synthetic peaks in the blue indicate that the synthetic spectrum is underblanketed. In the synthetic spectrum Na I and Ca II are detached at  $9000 \text{ km s}^{-1}$ , and an abrupt decrease in the Fe II line optical depths, by a factor of 10, has been introduced at  $10,000 \text{ km s}^{-1}$ . This is inferred to be a measure of the maximum velocity of the iron-peak core. The structure of the synthetic spectrum near  $5000\text{\AA}$  is quite sensitive to the velocity of the Fe II line optical depth discontinuity (Fisher 1998).

The major shortcoming in the upper panel of Figure 4 is that the broad minimum observed near  $7000\text{\AA}$  is not reproduced by the synthetic spectrum. (The weak synthetic absorptions in the vicinity are from Fe II.) A possible identification for this feature is [O II]  $\lambda\lambda 7320, 7330$  (Fisher 1998, Hatano et al. 1998). For a forbidden transition the natural first approximation to the source function would be the Planck function evaluated at the local

electron temperature, but instead of introducing a whole new fitting function involving the radial dependence of the electron temperature, we have simply retained the resonance scattering source function. In the lower panel of Figure 4 the [O II] feature is calculated with a line optical depth that is detached at  $10,000 \text{ km s}^{-1}$ , where  $\tau = 0.5$ , and has a shallow radial gradient ( $v_e = 20,000 \text{ km s}^{-1}$ ) such that  $\tau = 0.24$  at the maximum [O II] velocity of  $25,000 \text{ km s}^{-1}$ . The upper panel of Figure 5, which is like the upper panel of Figure 4 but with the [O II] feature included in the synthetic spectrum, looks better than the upper panel of Figure 4. The lower panel of Figure 5 shows how the fit degrades when Na I is not detached, the discontinuity in the Fe II line optical depths is not introduced, and the upper and lower velocity limits on [O II] are dropped.

From a spectroscopic point of view the [O II] identification is attractive and plausible. Moreover, Kirshner et al. (1993) discussed the velocity interval in which the O I  $\lambda 7773$  line could be detected in the early spectra of a small sample of well observed SNe Ia. For SN 1991T they estimated that the O I line had a significant optical depth from at least as low as  $9000 \text{ km s}^{-1}$  to at least as high as  $19,000 \text{ km s}^{-1}$ , which is not inconsistent with what we are using for [O II]. But the mass and associated kinetic energy of the oxygen that would be required to produce a significant [O II] line optical depth, at such high velocities and at this fairly late phase, appear to be high. For this feature, with its very low transition probability, just producing a uniform line optical depth of 0.2 requires

$$M = 0.26v_{25}^3t_{77}^2f_O^{-1}M_{\odot}; \quad E_K = 10^{51}v_{25}^5t_{77}^2f_O^{-1}\text{erg}$$

where  $v_{25}$  is the maximum velocity in units of  $25,000 \text{ km s}^{-1}$ ,  $t_{77}$  is the time since explosion in units of 77 days (allowing for a rise time to maximum of 18 days), and  $f_O$  is the fraction of all oxygen that is in the lower level of the transition. It is possible that essentially all of the oxygen is singly ionized at this phase, but  $f_O$  must be significantly less than unity

because the lower level of the transition is 3.3 eV above the ground level of singly ionized oxygen. (The ground level of the transition is, at least, the metastable lowest level of the doublets, the true ground level of singly ionized oxygen being a quartet.)

We have no plausible alternative to offer for the 7000Å minimum. If it is not an absorption feature at all, then the continuum must be at a level that is considerably lower than we have adopted to obtain the fits shown in the top panels of Figures 4 and 5. We suspect that the [O II] identification is correct, but in view of the mass and energy problem the maximum [O II] velocity may need to be somewhat lower than the 25,000 km s<sup>-1</sup> that we have used.

### 4.3. Summary of the Inferred Composition Structure

In Paper I we presented evidence for C II in SN 1990N at  $v > 26,000$  km s<sup>-1</sup>. It is thought that when SNe Ia are arranged in a sequence from powerful events like SN 1991T to weak ones like SN 1991bg, SN 1990N belongs on the powerful side (e.g., Phillips 1992; Nugent et al. 1995). One might then expect events that are weaker than SN 1990N to have unburned carbon extending down to velocities lower than 26,000 km s<sup>-1</sup>, and our SYNOW studies of other SNe Ia suggest that this generally is the case (Fisher 1998). Similarly, one might expect events like SN 1991T that are thought to be stronger than SN 1990N to have a minimum velocity of carbon that is higher than 26,000 km s<sup>-1</sup>. But in SN 1991T we find evidence for C II moving at least as slow as about 15,000 km s<sup>-1</sup>. At the same time, we find evidence that the iron-peak core of SN 1991T extended out to velocities at least as high as in SN 1990N and other SNe Ia. Independently, Mazzali et al. (1998) list outer velocities of the iron core for 14 SNe Ia, inferred from nebular-phase spectra, and they find that SN 1991T has the highest velocity in their sample. Thus SN 1991T seems to have had both slower unburned carbon and a faster iron-peak core than SN 1990N, with its

intermediate-mass elements being confined to an unusually narrower velocity interval.

Figure 6 shows the velocity at the photosphere as a function of time. The pause in the velocity decrease, around  $10,000 \text{ km s}^{-1}$ , presumably reflects an increase in the density or the opacity near the outer edge of the iron-peak core. Our combined constraints on the composition structure are shown in Figure 7. The inferred structure is not like any hydrodynamical model that has been published. A speculation about the cause of the peculiar composition structure of SN 1991T will be offered in Section 5, after the implication of the high luminosity of SN 1991T is considered in the next section.

## 5. The Luminosity of SN 1991T

NGC 4527, the parent galaxy of SN 1991T, is in the southern extension of the Virgo cluster complex. According to the Nearby Galaxies Catalogue (Tully 1988) it is a member of the same small group of galaxies (group 11 –4 in Tully’s notation) as NGC 4536 and NGC 4496, the parent galaxies of the normal Type Ia SNe 1981B and 1960F. These three galaxies have similar heliocentric radial velocities of 1730, 1866, and 1738  $\text{km s}^{-1}$ , respectively, and they are the three brightest galaxies in the group. On the sky, NGC 4527 is 1.9 degrees from NGC 4496 and only 0.6 degrees from NGC 4536. Peletier & Willner (1991) found nearly identical Tully–Fisher distances for NGC 4527 and NGC 4536. Independently, Pierce (1994) obtained nearly identical Tully–Fisher distance moduli for all three of these galaxies. Tully (1988), Tully, Shaya, and Pierce (1992), and Peletier & Willner (1991) all agreed that this galaxy group is on the near side of the Virgo cluster complex. Since then, Saha et al. (1996a) have determined a Cepheid–based distance modulus of  $\mu = 31.10 \pm 0.13$  for NGC 4536, and similarly Saha et al. (1996b) obtain  $\mu = 31.03 \pm 0.14$  for NGC 4496. Pending a direct Cepheid–based determination of the distance to NGC 4527, which is to be attempted (A. Saha 1998, personal communication), we assume here that the distance modulus to

NGC 4527 is  $\mu = 31.07 \pm 0.13$  ( $D = 16.4 \pm 1.0$  Mpc).

The magnitudes and luminosities of SNe 1960F, 1981B, and 1991T are compared in Table 1. The  $B$  and  $V$  peak apparent magnitudes are from Saha et al. (1996b), Schaefer (1995a), and Lira et al. (1998), respectively. The observed  $B$  and  $V$  magnitudes of SNe 1960F and 1991T were similar, while those of SN 1981B were about 0.5–0.6 mag fainter.

The extinction of these three events by dust in our Galaxy should be negligible (Burstein & Heiles 1982), but there are reasons to think that SN 1991T was significantly extinguished by dust in its parent galaxy. (1) In projection, at least, the event occurred near a spiral arm of low surface brightness in NGC 4527, an Sb galaxy that is very dusty and has a high inclination of 74 degrees. For a good photograph that shows the location of SN 1991T in NGC 4527, see Figure 1 of Schmidt et al. (1994). (2) Photometric and spectroscopic observations of SN 1991T at an age of 2–3 years have been interpreted by Schmidt et al. (1994) in terms of a light echo caused by dust in NGC 4527. (3) Interstellar lines of Ca II (Meyer & Roth 1991) and Na I (Smith & Wheeler 1991; Filippenko et al. 1992; Ruiz-Lapuente et al. 1992), at the redshift of NGC 4527, were detected in the spectra of SN 1991T. Values of the color excess that have been estimated on the basis of the strengths of the Na I lines include  $E(B - V) = 0.34$  by Ruiz-Lapuente et al. (1992) and 0.13–0.23 by Filippenko et al. (1992). Although these estimates are recognized to be uncertain, some significant amount of extinction is to be expected. (4) Mazzali et al. (1995) and Nugent et al. (1995) concluded from its spectral features that SN 1991T was hotter than normal SNe Ia, yet some of the broad-band colors of SN 1991T were observed to be redder than those of normal SNe Ia. Phillips et al. (1992) estimated  $E(B - V) = 0.13$  by assuming that the intrinsic  $B - V$  color at maximum light was like that of normal SNe Ia. The revised photometry of Lira et al. (1998) makes SN 1991T even redder than had been thought, with  $B_{max} - V_{max} = 0.19 \pm 0.03$ .

For SN 1991T we adopt  $E(B - V) = 0.2 \pm 0.1$ . For SN 1981B we use  $E(B - V) = 0.10 \pm 0.05$  (M. M. Phillips 1995, personal communication), and we assume that the extinction of SN 1960F was negligible (Schaefer 1996; Saha et al. 1996b). It may be worth noting that these estimates are in accord with the galaxy “dustiness” categories of van den Bergh & Pierce (1990), who put NGC 4496 in category 1 (“some dust visible”), NGC 4536 in category 2 (“dust easily visible”) and NGC 4527 in category 3 (“galaxy appears very dusty”); only 12 of the 230 galaxies in their sample were assigned to the very dusty category. With our adopted extinction estimates, the extinction-free apparent ( $B^0$  and  $V^0$ ) and absolute ( $M_B^0$  and  $M_V^0$ ) magnitudes of the normal SNe 1960F and 1981B become similar, while SN 1991T becomes brighter by 0.7–0.8 mag (see Table 1).

For the bolometric correction,  $M_{bol} - M_V$ , of normal SNe Ia such as 1981B and 1960F, we adopt  $0.1 \pm 0.1$  (Höflich 1995; Nugent et al. 1995; Branch et al. 1997). Even before being corrected for extinction, SN 1991T had a larger fraction of its energy in the near ultraviolet than do normal SNe Ia (Nugent et al. 1995; Schaefer 1995b; Branch et al. 1997), therefore a smaller fraction of its total flux was emitted in the  $B$  and  $V$  bands and its  $M_{bol} - M_V$  was more negative than that of normal SNe Ia. For SN 1991T we adopt  $M_{bol} - M_V = -0.1 \pm 0.1$ , which probably is conservative for the present argument. The bolometric absolute magnitude of SN 1991T then exceeds that of SN 1981B by  $0.95 \pm 0.37$  mag (where the uncertainty in the *difference* between the distance moduli of NGC 4527 and NGC 4536 has been neglected), and the luminosity of SN 1991T exceeds that of SN 1981B by a factor between 1.7 and 3.4, with the best estimate being a factor of 2.4 (see Table 1).

The peak luminosity of a Type Ia supernova can be written (Arnett 1982, Branch 1992)

$$L = \alpha R(t_r) M_{Ni} \tag{1}$$

where  $R$ , the instantaneous radioactivity luminosity per unit nickel mass at the time of

maximum light, is a known function of the rise time  $t_r$ ,  $M_{Ni}$  is the mass of ejected  $^{56}\text{Ni}$ , and  $\alpha$  is dimensionless and of order unity. For normal SNe Ia, such as SN 1981B, characteristic values of  $M_{Ni} = 0.6M_{\odot}$ ,  $t_r = 18$  days, and  $\alpha = 1.2$  (e.g., Höflich & Khokhlov 1996; Branch et al. 1997) give  $L = 2.03 \times 10^{43}$  ergs  $\text{s}^{-1}$ . This corresponds to a bolometric absolute magnitude  $M_{bol} = -19.57$ , a little brighter than, but not inconsistent with, the value implied by the Cepheid distance and the adopted extinction.

At first glance one might think that sufficient overluminosity of SN 1991T with respect to SN 1981B could be achieved with a Chandrasekhar mass, just by allowing the nickel mass to approach the Chandrasekhar mass in SN 1991T (i.e.,  $1.4/0.6 = 2.33$ , and we have estimated that SN 1991T was more luminous than SN 1981B by a factor of 2.4). However, there are severe problems with this simple picture, in which nearly all of the ejected mass of SN 1991T is initially in the form of  $^{56}\text{Ni}$ . (1) Spectral lines formed by elements other than nickel, cobalt, and iron show that the initial composition of SN 1991T was not just  $^{56}\text{Ni}$ . (2) No hydrodynamical models of Chandrasekhar-mass explosions produce just  $^{56}\text{Ni}$ . Even the pure detonation model of Khokhlov et al. (1993) produced only  $0.92 M_{\odot}$  of  $^{56}\text{Ni}$ , with the rest of the mass being in the form of other iron-peak isotopes. (3) A rapid expansion of the ejecta caused by the high kinetic energy per gram, together with the prompt escape of gamma rays emitted by  $^{56}\text{Ni}$  in the outer layers, would make the light curve too fast, and with gammas escaping the value of  $\alpha$  would be low. For example, for the detonation model of Khokhlov et al. (1993), Höflich & Khokhlov (1996) calculated  $\alpha = 0.76$  (in their notation it is  $Q$ ). (5) The optical and gamma-ray luminosities depend on distance in the same way. From the optical brightness of SN 1991T and the lack of detection of gamma rays by Lichti et al. (1994) and Leising et al. (1995), the latter authors conclude that “some way of producing optically brighter but gamma-ray fainter supernovae [compared to SN Ia models in the literature] is required to explain SN 1991T”. A Chandrasekhar-mass explosion that contained nearly a Chandrasekhar mass of  $^{56}\text{Ni}$  would have a *low* ratio of



optical and gamma-ray luminosities.

If SN 1991T is at the same distance as SNe 1981B and 1960F then it is unlikely that its luminosity can be explained in terms of a Chandrasekhar mass ejection.

## 6. Discussion

If the luminosity of SN 1991T was too high to be explained in terms of a Chandrasekhar mass ejection, the only recourse would seem to be to appeal to the explosion of a super-Chandrasekhar product of the merger of two white dwarfs. The question of whether mergers of white dwarfs actually can produce explosions is not yet settled (e.g., Mochkovitch, Guerrero, & Segretain 1997). An attractive recent suggestion was that of Iben (1997), who noted that because tidal torques will spin up the premerger white dwarfs to rotate in near synchronism with the orbital motion, huge shear forces will arise at the onset of the merger. If both white dwarfs ignite prior to or during the merger, owing to shear and tidal heating, or if the ignition of one of the white dwarfs then provokes the ignition of the other, this might be a way to get not only a super-Chandrasekhar mass ejection, but even a super-Chandrasekhar mass of  $^{56}\text{Ni}$  if such should prove to be required. Getting a super-Chandrasekhar mass of  $^{56}\text{Ni}$  out of a thermonuclear explosion was difficult to envision before Iben’s suggestion. It must be noted, though, that in the first calculations of tidal heating during a merger, it failed by a narrow margin to cause carbon to ignite (Iben & Tutukov 1998).

It is interesting that on the basis of their population-synthesis studies, Tutukov & Yungelson (1994) predict that for “young” mergers, those that occur within 300 Myr of star formation, the average combined mass is substantially super-Chandrasekhar, typically about  $2.1 M_{\odot}$  (see their Figure 4). Recall that SN 1991T appears to have occurred near a

spiral arm. Preliminary indications are that the several other events resembling SN 1991T that have been discovered in recent years also tend to be associated with star forming regions and/or to be significantly extinguished by dust (A. V. Filippenko 1998, personal communication; P. Garnavich 1998, personal communication). SN 1991T–type events may be from a younger population than most SNe Ia.

It also is interesting that Ruiz–Lapuente et al. (1992) discuss the possible detection of a narrow circumstellar line of O I  $\lambda$ 8446 in their earliest spectrum of SN 1991T. Searching for narrow circumstellar lines of hydrogen, helium, carbon, or oxygen is one the best ways to probe the composition of the donor star in the binary progenitor system of a SN Ia (Branch et al. 1995). No signs of circumstellar interaction, and no clear detections of narrow circumstellar lines of hydrogen or helium have been found in *any* SN Ia.

The proposition that SN 1991T was the result of a super–Chandrasekhar merger is consistent with the findings of Höflich & Khokhlov (1996), who calculated light curves for a variety of SN Ia hydrodynamical models and found that the slow light curve of SN 1991T was best fit by models of Khokhlov et al. (1993) that had a super–Chandrasekhar ejecta and/or substantial amounts of unburned carbon and oxygen in their outermost layers. The particular models that Höflich & Khokhlov cited as best fitting the light curve have a peak  $M_V \simeq -19.4$ , which is not luminous enough for SN 1991T. However, in their models the underlying explosion was the detonation of only  $1.2 M_\odot$ , inside low–density carbon–oxygen envelopes of  $0.2$ ,  $0.4$ , and  $0.6 M_\odot$ . If the central explosion had been the detonation of a Chandrasekhar mass the peak would have been brighter.

In a very general sense, the composition structure expected of a merger explosion might resemble the composition structure that has been inferred for SN 1991T (cf. Ruiz–Lapuente et al. 1992). An unusually strong explosion produces a high–mass, high–velocity iron–peak core surrounded by an unusually small mass of intermediate–mass

elements; this encounters a surrounding low-density mass of carbon and oxygen which decelerates the intermediate-mass elements and forces them into a narrow velocity interval. The super-Chandrasekhar models of Khokhlov et al. (1993) had this sort of composition structure, but the minimum velocity of unburned carbon was lower than  $10,000 \text{ km s}^{-1}$ , a value which is lower than we infer from the spectra. In this respect, too, replacing the  $1.2 M_{\odot}$  core with a Chandrasekhar mass would be a step in the right direction. None of this explains the presence of iron-peak elements at higher velocity than the intermediate-mass elements, or the possible coexistence in velocity space of iron-peak elements and unburned carbon. Eventually, only multidimensional hydrodynamical studies of the merger process can tell us whether this is possible.

It should be noted that Liu, Jeffery & Schultz (1997b) used a steady-state model of ionization and thermal structure to calculate early nebular-phase spectra for comparison with observed spectra obtained hundreds of days after the explosion. Although they favored a *sub*-Chandrasekhar mass ejection for SN 1991T, the mass was higher than they favored for normal SNe Ia (Liu, Jeffery, & Schultz 1997a).

The argument that SN 1991T was super-Chandrasekhar depends, of course, on our assumption that SN 1991T is at the same distance as SNe 1981B and 1960F. A Cepheid-based determination of the distance to NGC 4527, although perhaps not easy for such a dusty, inclined galaxy, is vital to check on this assumption.

This work has been supported by NSF grants AST 9417102, 9417242, and 9731450 and NASA grant NAG 5-3505.

## REFERENCES

- Arnett, W. D. 1982, *ApJ*, 253, 785
- Branch, D. 1992, *ApJ*, 392, 35
- Branch, D., Fisher, A., and Nugent, P. 1993, *AJ*, 106, 2383
- Branch, D., Nugent, P., and Fisher, A. 1997, in *Thermonuclear Supernovae*, ed. P. Ruiz-Lapuente, R. Canal, and J. Isern (Kluwer, Dordrecht), p. 715
- Branch, D. Livio, M., Yungleson, L. R., Boffi, F. R., and Baron, E. 1995, *PASP* 107, 1019
- Burstein, D., and Heiles, C. 1982, *ApJS*, 54, 33
- Filippenko, A. V. et al. 1992, *ApJ*, 384, L15
- Fisher, A. 1998. PhD thesis. University of Oklahoma
- Fisher, A., Branch, D., Nugent, P., and Baron, E. 1997, *ApJ*, 481, L89
- Hatano, K., Branch, D., Fisher, A., and Baron, E. 1998, *ApJS*, submitted
- Hauschildt, P. and Baron, E. 1998, *J. Comp and Applied Math.*, in press
- Höflich, P. 1995, *ApJ*, 443, 89
- Höflich, P. and Khokhlov, A. 1996, *ApJ*, 457, 500
- Iben, I., Jr. 1997, in *Thermonuclear Supernovae*, eds. P. Ruiz-Lapuente, R. Canal, & J. Isern (Dordrecht, Kluwer), p. 111
- Iben, I., Jr., and Tutukov, A. V. 1998, *ApJ*, in press
- Jeffery, D. J., Leibundgut, B., Kirshner, R. P., Benetti, S., Branch, D., & Sonneborn, G. 1992, *ApJ*, 397, 304
- Khokhlov, A., Müller, E., and Höflich, P. 1993, *A&A*, 270, 223.
- Kirshner, R. P. et al. 1993, *ApJ*, 415, 589

- Leibundgut, B., Kirshner, R. P., Filippenko, A. V., Shields, J. C., Foltz, C. B., Phillips, M. M., & Sonneborn, G. 1991, *ApJ*, 371, L23
- Leising, M. D. et al. 1995, *ApJ*, 450, 805
- Lichti, G. G., et al. 1994, *A&A*, 292, 569
- Lira, P. et al. 1998, *AJ*, 115, 234
- Liu, W., Jeffery, D. J., and Schultz, D. R. 1997a, *ApJ*, 483, L107
- Liu, W., Jeffery, D. J., and Schultz, D. R. 1997b, *ApJ*, 486, L35
- Mazzali, P. A., Cappellaro, E., Danziger, I. J., Turatto, M., & Benetti, S. 1998, astro-ph/9803229
- Mazzali, P. A., Danziger, I. J., and Turatto, M. 1995, *MNRAS*, 297, 509
- Meyer, D. M., & Roth, K. C. 1991, *ApJ*, 383, L41
- Mochkovich, R., Guerrero, J., & Segretain, L. 1997, in *Thermonuclear supernovae*, ed. P. Ruiz-Lapuente, R. Canal, & J. Isern (Kluwer, Dordrecht), p. 187
- Nomoto, K., Thielemann, F.-K., & Yokoi, K. 1984, *ApJ*, 286, 644
- Nugent, P., Phillips, M., Baron, E., Branch, D., & Hauschildt, P. 1995, *ApJ* 455, L147
- Peletier, R. F., & Willner, C. P. 1991, *ApJ*, 382, 382
- Phillips, M. M. et al. 1992, *AJ*, 103, 1632
- Pierce, M. J. 1994, *ApJ*, 430, 53
- Ruiz-Lapuente, P. et al. 1992, *ApJ*, 387, L33
- Saha, A., Sandage, A., Labhardt, L., Tammann, G. A., Macchetto, F. D., & Panagia, N. 1996a, *ApJ*, 466, 55
- Saha, A., Sandage, A., Labhardt, L., Tammann, G. A., Macchetto, F. D., & Panagia, N. 1996b, *ApJS*, 107, 693

- Schaefer, B. E. 1995a, ApJ, 449, L9
- Schaefer, B. E. 1995b, ApJ, 450, L5
- Schaefer, B. E. 1996, ApJ, 460, L19
- Schmidt, B. P., et al. 1994, ApJ, 434, L19
- Smith, V. & Wheeler, J. C. 1991, IAU Circ., No. 5256
- Thielemann, F.–K., Nomoto, K., & Yokoi, K. 1986, A&A, 158, 17
- Tully, R. B. 1988, Nearby Galaxies Catalogue (Cambridge University Press, Cambridge)
- Tully, R. B., Shaya, E. J., & Pierce, M. J. 1992, ApJS, 80, 479
- Tutukov, A. V., & Yungelson, L. R. 1994, MNRAS, 268, 871
- van den Bergh, S., & Pierce, M. J. 1990, ApJ, 364, 444
- Yamaoka, H., Nomoto, K., Shigeyama, T., & Thielemann, F.–K. 1992, ApJ, 393, L55

Fig. 1.— A spectrum of SN 1991T obtained at  $-13$  days (Phillips et al. 1992) is compared to a synthetic spectrum that has  $v_{phot} = 15,000 \text{ km s}^{-1}$  and  $T_{exc} = 13,000 \text{ K}$ . Ions responsible for features in the synthetic spectrum are marked.

Fig. 2.— A spectrum of SN 1991T obtained at  $-4$  days (Phillips et al. 1992) is compared to a synthetic spectrum that has  $v_{phot} = 10,000 \text{ km s}^{-1}$  and  $T_{exc} = 13,000 \text{ K}$ . Ions responsible for features in the synthetic spectrum are marked.

Fig. 3.— A spectrum of SN 1991T obtained at  $+6$  days (Phillips et al. 1992) is compared to synthetic spectra that have  $v_{phot} = 9500 \text{ km s}^{-1}$  and  $T_{exc} = 10,000 \text{ K}$ . Ions responsible for features in the synthetic spectrum are marked. In the upper panel, maximum velocities of  $12,000$  and  $15,000 \text{ km s}^{-1}$  have been imposed on S II and Si II, respectively. In the lower panel these limits have been removed.

Fig. 4.— A spectrum of SN 1991T obtained at  $+59$  days (W. P. S. Meikle et al., unpublished) is compared to synthetic spectrum that have  $v_{phot} = 4000 \text{ km s}^{-1}$  and  $T_{exc} = 10,000 \text{ K}$ . In the synthetic spectrum of the upper panel, one feature is produced by Na I (detached at  $9000 \text{ km s}^{-1}$ ), two features are produced by Ca II, and all others are produced by Fe II (which has an abrupt factor of ten decrease in its optical depths at  $10,000 \text{ km s}^{-1}$ ). In the synthetic spectrum of the lower panel, the one feature is produced by [O II].

Fig. 5.— A spectrum of SN 1991T obtained at  $+59$  days (W. P. S. Meikle et al., unpublished) is compared to synthetic spectrum that have  $v_{phot} = 4000 \text{ km s}^{-1}$  and  $T_{exc} = 10,000 \text{ K}$ . The synthetic spectrum of the upper panel is like the one in the upper panel of Figure 4, but now [O II] is included. In the synthetic spectrum of the lower panel, the detachment of Na I and Ca II, the Fe II optical depth discontinuity, and the velocity limits on [O II] have been removed.

Fig. 6.— The velocity at the photosphere, used in the synthetic spectra, is plotted against time.

Fig. 7.— Inferred constraints on the composition structure. Solid arcs indicate maximum or minimum velocities that were imposed in the spectrum calculations; for example, a maximum velocity of  $15,000 \text{ km s}^{-1}$  was imposed on silicon. Dashed arcs merely indicate maximum or minimum velocities at which the element could be detected; for example, calcium could be detected up to  $18,000 \text{ km s}^{-1}$  but there is no evidence against its presence at higher velocities. For Fe II, the transition from a solid line to a dotted one is at the velocity at which the optical depth discontinuity was introduced.



Table 1. Luminosities of Three Type Ia Supernovae

|                              | SN 1960F          | SN 1981B          | SN 1991T          |
|------------------------------|-------------------|-------------------|-------------------|
| galaxy                       | NGC 4496          | NGC 4536          | NGC 4527          |
| $B$                          | $11.60 \pm 0.10$  | $12.04 \pm 0.04$  | $11.70 \pm 0.02$  |
| $V$                          | $11.51 \pm 0.15$  | $11.98 \pm 0.04$  | $11.51 \pm 0.02$  |
| $E(B - V)$                   | $0.0 \pm 0.00$    | $0.10 \pm 0.05$   | $0.20 \pm 0.10$   |
| $B^0$                        | $11.60 \pm 0.10$  | $11.63 \pm 0.20$  | $10.88 \pm 0.41$  |
| $V^0$                        | $11.51 \pm 0.15$  | $11.67 \pm 0.16$  | $10.89 \pm 0.31$  |
| $M_B^0$                      | $-19.43 \pm 0.14$ | $-19.47 \pm 0.24$ | $-20.19 \pm 0.43$ |
| $M_V^0$                      | $-19.56 \pm 0.20$ | $-19.43 \pm 0.21$ | $-20.18 \pm 0.34$ |
| $M_{bol} - M_V$              | $0.10 \pm 0.10$   | $0.10 \pm 0.10$   | $-0.10 \pm 0.10$  |
| $M_{bol}$                    | $-19.46 \pm 0.22$ | $-19.33 \pm 0.23$ | $-20.28 \pm 0.35$ |
| $L/10^{43} \text{ergs}^{-1}$ | $1.85 \pm 0.43$   | $1.63 \pm 0.38$   | $3.93 \pm 1.54$   |

Fig 1

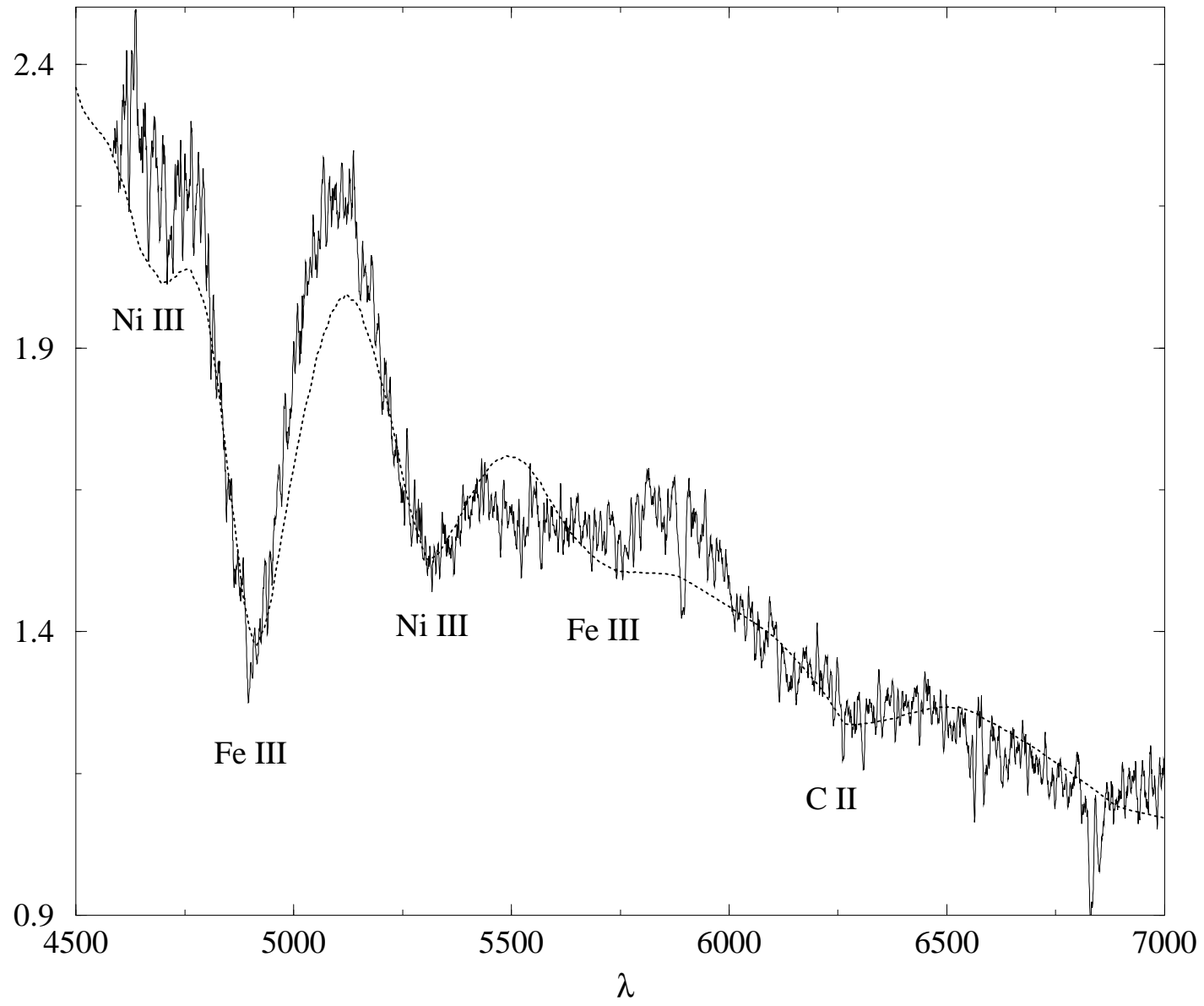


Fig 2

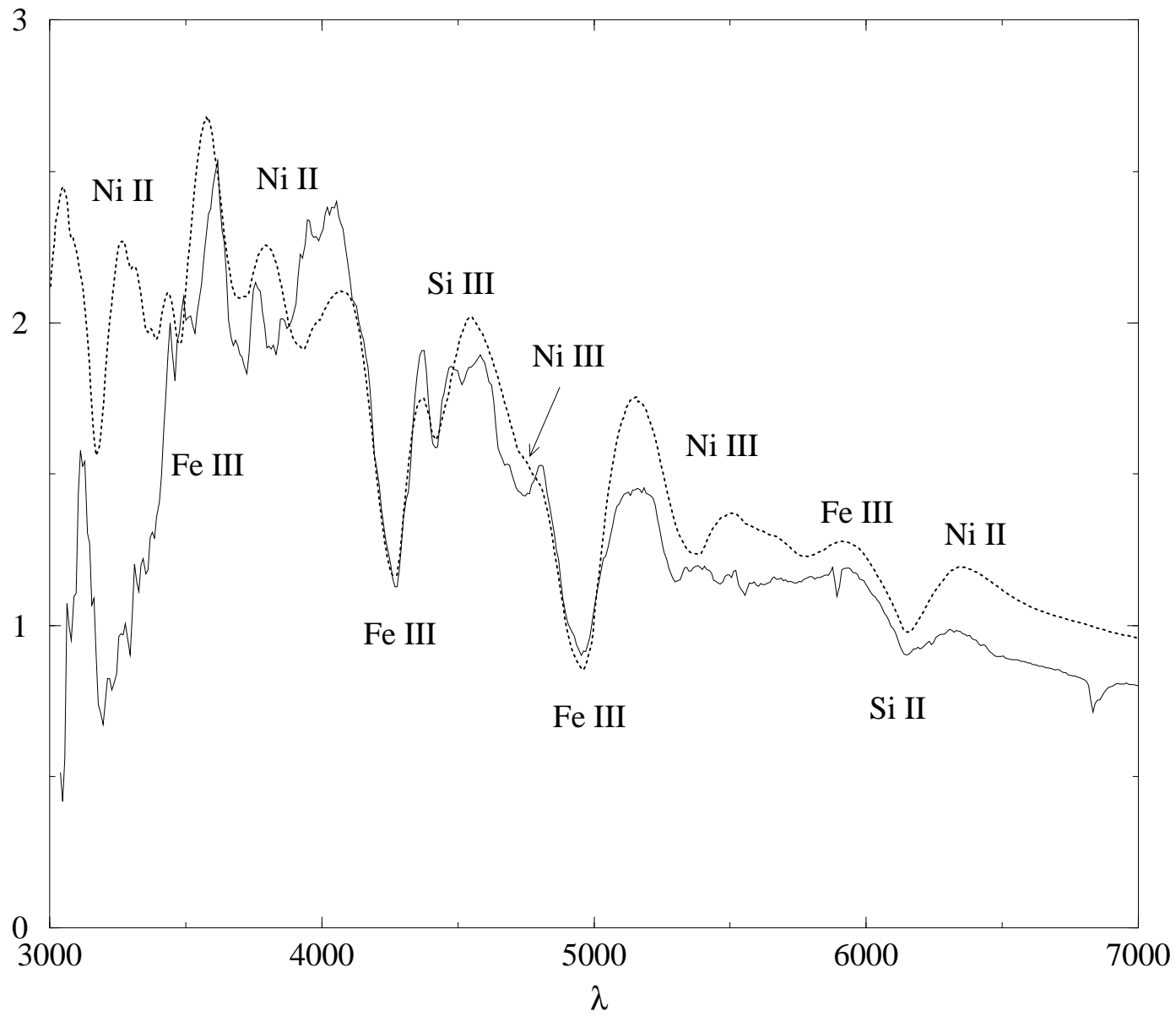


Fig 3

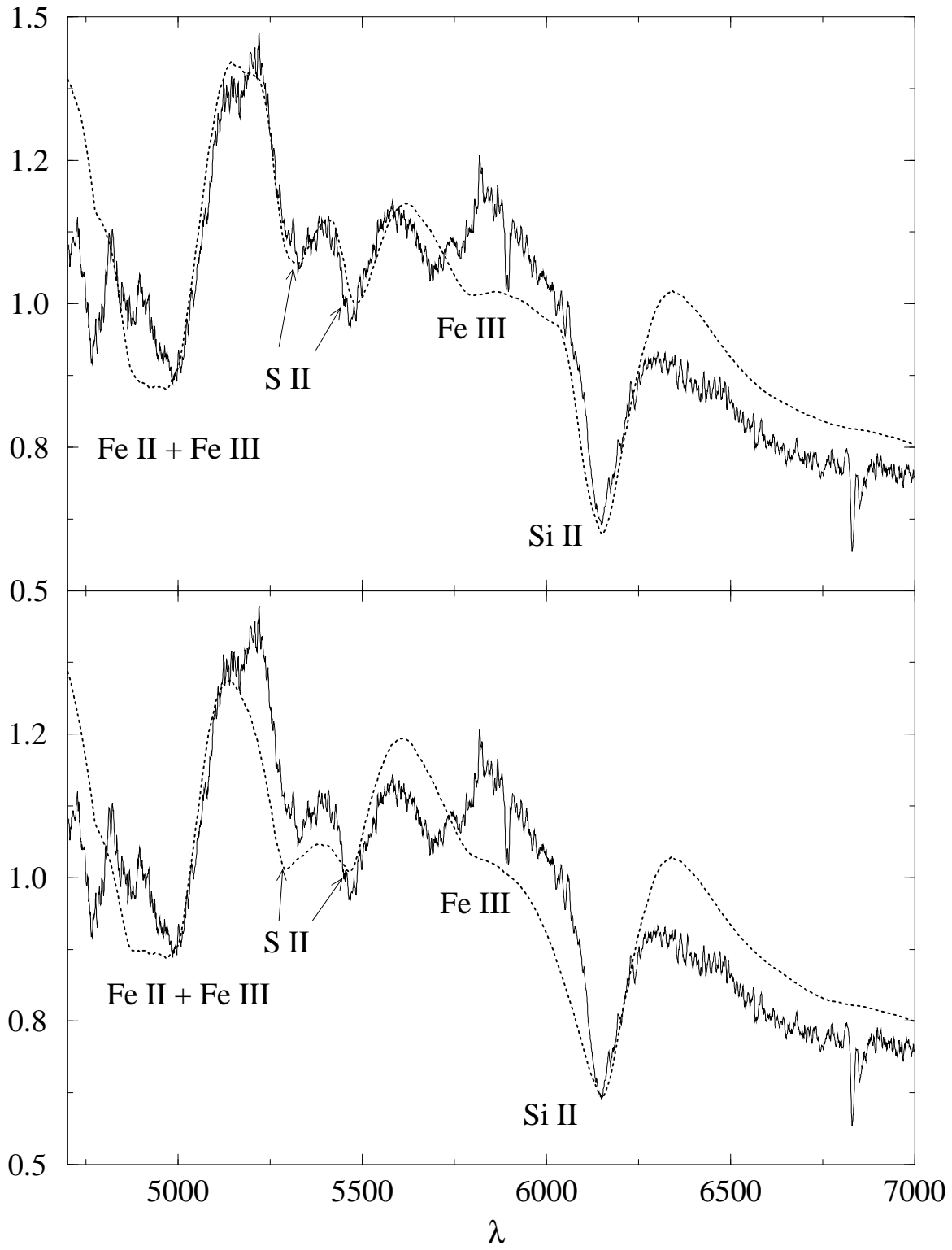


Fig 4

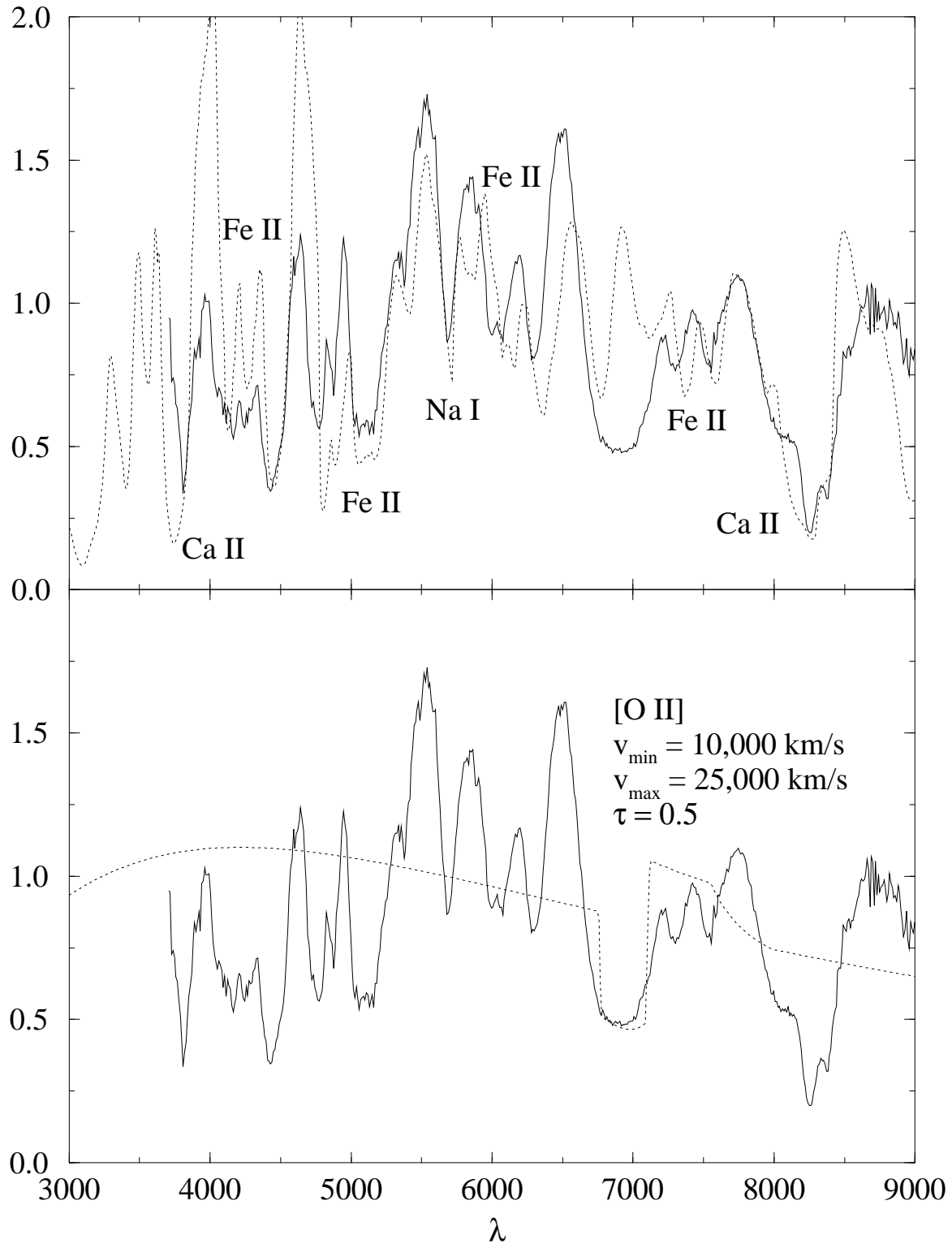


Fig 5

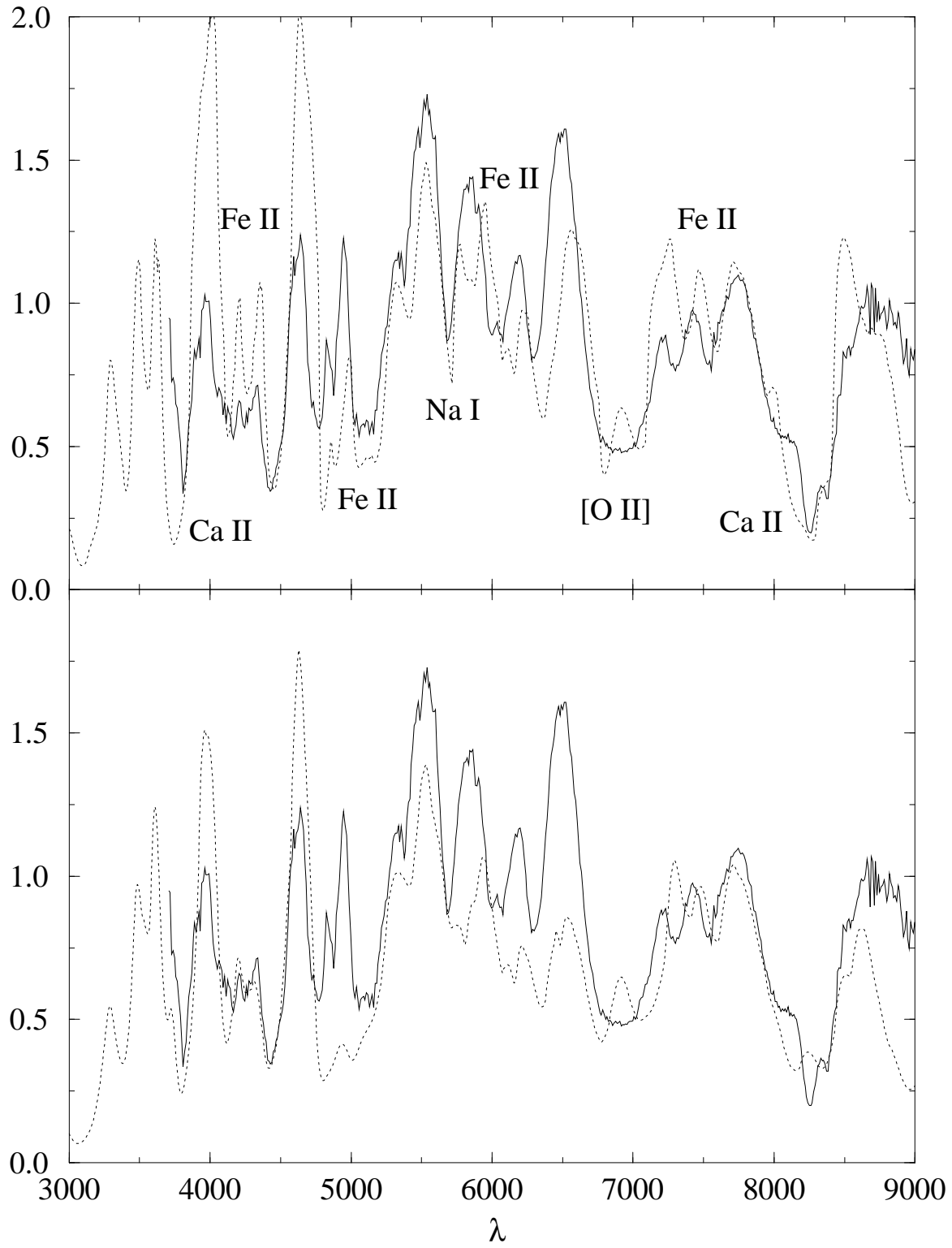


Fig 6

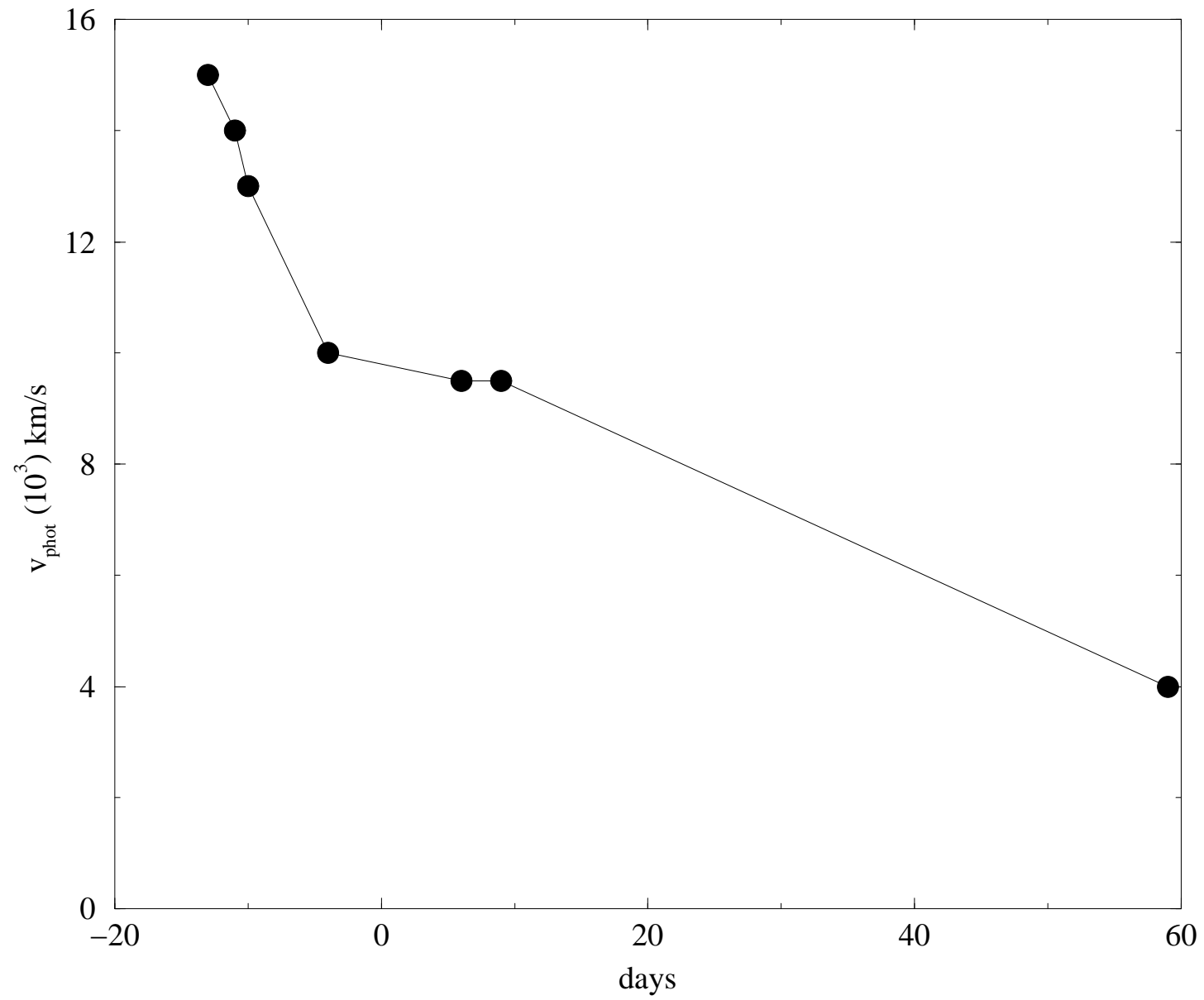


Fig 7

